

Cancer Immunotherapy Preparation and Immune Cells Activation through Hapten-Enhanced Chemotherapy in Primary Lung Cancer

Baofa Yu^{1,2,3,4,5*}, Feng Gao¹, Peng Jing¹, Peicheng Zhang¹, Xiaomin Zhang¹, Guoqin Zheng¹, Shengjun Zhou¹, Jian Zhang², Fu Qiang², Yan Han², Yan Jiang⁶

¹Department of Oncology, TaiMeiBaofa Cancer hospital, Dongping, Shandong Province, China; ²Department of Oncology, Jinan Baofa Cancer Hospital, Jinan, Shandong Province, China; ³Department of Oncology, Beijing Baofa Cancer Hospital, Beijing, China; ⁴Department of Oncology, Immune Oncology System, San Diego, California, USA; ⁵Department of Oncology, Huanan Hospital, Shenzhen University, Shenzhen, Guangdong, China; ⁶Department of Oncology, Singleron Biotechnologies, Woodbridge, Connecticut, USA

ABSTRACT

Immunotherapy is a novel treatment of lung cancer. However, still lacking of method to awake of immune cell into fighting posture since most of patients got the standard of care with concurrent chemo or radiotherapy. Comparative studies on the single-cell level of immune reaction-related abscopal effect in untreated tumors before and after the major tumor with chemotherapeutic drugs plus hapten. Using Single-cell RNA sequencing (scRNA-seq) analyze the changes at the molecular level of tumor reflection from the treated major tumor. It was found that immunity reaction activated like Mononuclear Phagocytes [MP's], mature DC cells and T and NK cells including CD8+ effector T cells, CD8Trm, NK cells, also awaking memory T cells, CD8+ effector T cells, CD8Trm and Naive T increased in untreated tumor after major tumor treated. It can be induced through intratumoral injection of cytotoxic drug plus hapten, vital in modifying Associate Tumor Antigens (ATAs) to improve neu ATAs. Our study provides evidence that hapten mediated local chemotherapy is safe and

effective method while it induces a systematic immunity against cancer by initiating immune response from the endometrial cancer to achieve desirable clinical outcome in order to prevention of tumor cell metastasis with or without hysterectomy, in fact, it bring the immunotherapy advance ahead any treatment of cancer, cleverly integrated into existing therapies and make those quite effective in prolong patient's life.

Key Words: Hapten; Immunotherapy; Lung cancer; Chemotherapy

Correspondence:

Baofa Yu, Department of Oncology, TaiMeiBaofa Cancer hospital, Dongping, Shandong Province, China, Tel +86 105 615 2159; E-mail: bfyuchina@126.com

INTRODUCTION

Lung cancer remains the leading cause of cancer mortality in the United States and worldwide [1]. Patients with metastasis Non-Small-Cell Lung Cancer (mNSCLC) is difficult to treat, Immune Checkpoint Inhibitors (ICIs), specific antibodies against the programmed death (PD-1) receptor, Programmed Death-Ligand 1 (PD-L1) in the therapeutic strategy of mNSCLC either in first- or in second-line option have led to prolonged survival of a proportion of these patients. Although a unique set of immune-mediated adverse events, such as pneumonitis, has been observed [2]. Unlike the current therapies of as chemotherapy, radiotherapy, or targeted therapy that target tumor cells, also damage the immune cells, PD1 or PD-L1 directly restore the exhausted host antitumor immune responses mediated by the tumors. However, the survival benefit granted by immunotherapy in this setting, only 1/3 of patients are alive and disease free at 5 years, since most of patients got the standard of care with Concurrent Chemo or Radiotherapy (CCRT), the patient's immune system was damaged to a low of function of immune cells like T cells in Weak to Sick (WtoS) condition, ICIs cannot take place to strength the weak to sick T cell fighting tumor cells [3]. To improve the situation of WtoS T cell is very important for clinical benefit, clinical practice should except to avoid higher dose of chemotherapy or radiation therapy for those patient with CCRT, we had tried to find a method to awaken the immune cells in fighting posture from the primary mNSCLC treated by Hapten Enhanced Local Chemotherapy (HELIC) and make a patient's immune system ready for ICIs therapy by hapten sensitized the immune cell to tumor cell [4,5].

Hapten plus cytotoxic drugs have been successfully injected into the tumor to treat lung cancer, extending the survival time of patients. Hapten plays immuno-modulators to modify the epitopes of tumor antigens released from death tumor cells after HELIC and produces an immune response of the tumor, it resulted in prolonged survival time of cancer patients [4,5]. These previous results point toward the rationale that the increase of immunity reaction may be related to the abscopal effect induced by hapten and prolonged survival time [6]. It may also benefit to ICIs therapy since immune cells was awakened to good state from WtoS condition.

In order to check the immune cells status after treatment, we applied scRNA-seq to two samples of tumor tissues from lung cancer before and after primary lung cancer treated by HELIC. Through comparative analysis between two samples and subsets of lung cancer, we comprehensively described the expression characteristics of malignant epitheliums and immune cells including myeloid cell sand platelets, as well as the dynamic changes of cell percentages, and the heterogeneity of cell subtypes which all relates to the immune cells state as a potential abscopal effect to fighting cancer cells or as basic ground for ICIs to strength T cell [6,7].

The immunity reaction was detected and compared the molecular changes by scRNA-seq and made ready for cancer immunotherapy like PD1 or PD-L1. The outcomes of these proposed aims may provide the detailed understanding of immune cell awakened at molecular base in fighting posture from the lung cancer treated by HELIC and may develop a more reliable, hapten enhanced sensitization immunotherapy for cancer patients.

MATERIALS AND METHODS

Patient treatment and clinical specimens

The patient had a clinical diagnosis with pathological diagnosis as adenocarcinoma of the lung cancer, and met the indications for HELIC treatment, signed the informed consent form, and this experiment was approved by the Ethics Committee Board of Shandong Baofa Cancer

This is an open access article distributed under the terms of the Creative Commons Attribution Noncommercial Share Alike 3.0 License, which allows others to remix, tweak, and build upon the work non commercially, as long as the author is credited and the new creations are licensed under the identical terms.

For reprints contact: Pharmacy@jbclinpharm.org

Received: 12 Jul, 2023; Manuscript No. jbcinphar-23-106204; **Editor Assigned:** 14 Jul, 2023, Pre QC No. jbcinphar-23-106204; **Reviewed:** 21 Jul, 2023, QC No. jbcinphar-23-106204; **Revised:** 4 Aug, 2023, Manuscript No. jbcinphar-23-106204; **Published:** 11 Aug, 2023. DOI: 10.37532/0976-0113.14(S1).18

Cite this article as: Yu B, Gao F, Jing P, et al. Cancer Immunotherapy Preparation and Immune Cells Activation through Hapten-Enhanced Chemotherapy in Primary Lung Cancer. J Basic Clin Pharma. 2023,14(S1):10-16.

Institute (TMBF 0010, 2015) for therapy and participation in the study prior to either commencing, and also, all method for experiments were performed in accordance with relevant guidelines and regulations.

The treatment was performed at Taimei Cancer Hospital by HELC to the lung tumor site by the spine needle under CT guiding [4-6]. Surgical biopsy samples were collected from lung tumor on the day before treatment and a second surgical biopsy were performed one weeks later following the first treatment. Once the lung tumor samples were surgically removed, it was immediately stored in sCellLiVE® Tissue Preservation Solution (Singleron) and taken back to the laboratory for further processing. The patient started to have normal dose of PD1 PD-1 inhibitor Carrilizumab (Jiangsu Hengrui) therapy, 200mg intravenously twice at day 1 and day 7, at same time another patient without HELC pretreatment also had PD-1 inhibitor Carrilizumab (Jiangsu Hengrui) therapy, 200mg intravenously twice at day 1 and day 7, following to monitoring the response and tumor size by CT (Figure 1a-1g).

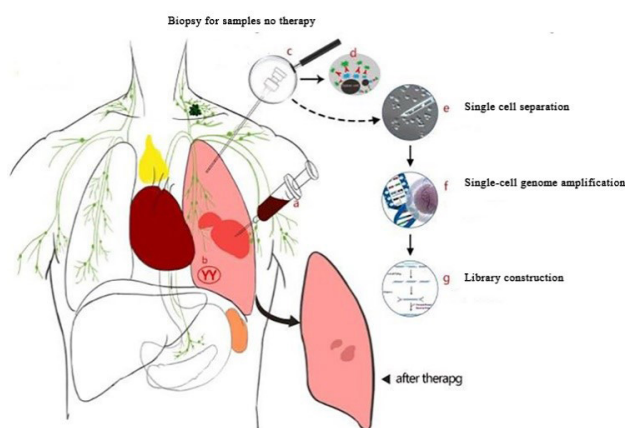


Figure 1: Graphic abstract of schematic diagram of single-cell sequencing process for lung cancer. (A) Syringe for injection with chemotherapy drug plus hapten into primary tumor in the scope of big tumor area, cause the tumor cell death, necrosis with inflammation, there is an haptenization with the tumor antigen released from death tumor cells be strong tumor antigens as neu tumor antigens (TAA) while DC cell capture the neu tumor antigens for antigen presentation process; (B) After DC cell capture the neu tumor antigens for antigen presentation process, the immune system of patient body produce the immunity reaction related whole body immunological response to tumor; (C): Thymus and spleen involved in the immune reaction to produce cytokines and antibodies from immune system and can circulate in the blood to find the tumor where the metastasis cell was, like metastasis in the lymph node, and bind the antigen on the tumor cell membrane or nuclear of metastasis to make the changes at molecular level in sentinel lymph node as a window for watching; (D) Using surgical biopsy to take a small part of lymph node at Supraclavicular lymph nodes before and after intra-tumoral injection to the primary pancreatic tumor in order to evaluate the changes of sentinel lymph node at molecular level; (E) After took the tumor tissue, immediately brought to the laboratory and tissue disassociation for cell separation; (F) : Analysis of single cell genome application profile; (G) Genome library construction.

Tissue disassociation and cells collection

After the fresh tissue samples were surgically obtained, fresh tissue samples were surgically obtained and stored in the sCellLiVE® Tissue Preservation Solution (Singleron) on ice. First, the tissue samples were washed with Hanks Balanced Salt Solution (HBSS) After with small tissue pieces were transferred to a 15-ml centrifuge tube and digested using sCellLiVE® Tissue Dissociation Solution (Singleron) under shaking conditions at 37°C for 15 min. Then, the samples were filtered with 40 µm sterile strainers, and centrifuged at 1,000 rpm at 4°C for

5 min. Next, 2 ml GEXSCOPE® Red Blood Cell Lysis Buffer (RCLB, Singleron) was added to lyse the red blood cells for 10 min. Finally, the single cell suspension was collected after re-suspension with Phosphate Buffered Saline (PBS), and trypan blue (Sigma) staining was used to calculate cell activity and cell count under a microscope.

Single-Cell RNA Sequencing

Single-cell suspensions ($1\sim3\times10^5$ cells/mL) with PBS (HyClone) were loaded onto microwell chip using the Singleron Matrix® Single Cell Processing System. Briefly, the scRNA-seq library was constructed using the GEXSCOPE® Single Cell RNA Library Kits (Singleron) and according to the operating instructions. The library was lastly sequenced with 150 bp was diluted to 4nM and paired-end reads on the IlluminaHiSeq X platform.

Sequencing data processing and quality control

The original gene expression matrix data were generated using the CeleScopeR (<https://github.com/singleron-RD/CeleScope>) software. CeleScopeR is a single-cell data processing software developed by Singleron that can execute a series of standard analysis procedures and can finally display the gene expression matrix required for downstream analysis. Briefly, after using fastqc (version 0.11.7) and cutadapt (version 1.17) to quality control and filter the data, reads were compared with the reference genome GRCh38 with ensemble version 93 gene annotation using STAR (version 2.6.1b)[8,9]. Then, featureCounts (version 1.6.2) was used to output the gene count matrix. The Seurat program (<http://satijalab.org/seurat>, R package, v.3.0.1) was used for cell type identification and cluster analysis of RNA sequencing data. The expression matrix was imported into R by the read, table function, and the cell cluster was analyzed by the FindCluster function (parameter resolution 0.6).

Differentially Expressed Genes (DEGs) analysis

To identify Differentially Expressed Genes (DEGs), we used the scanpy. `tl.rank_genes_groups` function based on Wilcoxon rank sum test with default parameters, and selected the genes expressed in more than 10% of the cells in both of the compared groups of cells and with an average log (Fold Change) value greater than 1 as DEGs. Adjusted p value was calculated by benjamini-hochberg correction and the value 0.05 was used as the criterion to evaluate the statistical significance.

Cell type annotation

The cell type identity of each cluster was determined with the expression of canonical markers found in the DEGs using SynEcoSys database (Singleron Biotechnologies). Heatmaps/dot plots/violin plots displaying the expression of markers used to identify each cell type were generated by scanpy inbuilt functions and ggplot2.

Single-Cell Copy Number Variation (CNV) analysis

The InferCNV package was used to detect the CNAs in malignant cells. Non-malignant cells (T and NK cells) were used as control references to estimate the CNVs of malignant cells. Genes expressed in more than 20 cells were sorted based on their loci on each chromosome. The relative expression values were centered to 1, using 1.5 standard deviation from the residual-normalized expression values as the ceiling. A slide window size of 101 genes was used to smooth the relative expression on each chromosome, to remove the effect of gene-specific expression.

Pathway enrichment analysis

To investigate the potential functions of DEGs between clusters, the Gene Ontology (GO) and Kyoto Encyclopedia of Genes and Genomes (KEGG) analysis were used with the “clusterProfiler” R package 3.16.1

[10]. GO gene sets including Molecular Function (MF), Biological Process (BP), and Cellular Component (CC) categories were used as reference. Pathways with p_{adj} value less than 0.05 were considered as significantly enriched.

Trajectory analysis

Monocle 2 algorithm: was used for pseudo-time trajectory analysis, and the dimensionality reduction method used was DDRTree [11].

Intra-Tumoral Heterogeneity (ITH) score calculation

The ITH score was defined as the average Euclidean distance between the individual cells and all other cells, in terms of the first 20 principal components derived from the normalized expression levels of highly variable genes. The highly variable gene was identified using the "FindVariableGenes" function in the Seurat package, with default parameters.

Cell-cell interaction analysis (CellPhoneDB)

Cell-cell interaction (CCI) between B cells, Epithelial cells, Fibroblasts,

Mononuclear phagocytes, Mast cells, Neutrophils, T and NK cells were predicted based on known ligand-receptor pairs by Cellphone DB v2.1.0 [12]. Permutation number for calculating the null distribution of average ligand-receptor pair expression in randomized cell identities was set to 1000. Individual ligand or receptor expression was thresholded by a cutoff based on the average log gene expression distribution for all genes across each cell type. Predicted interaction pairs with p value < 0.05 and of average log expression > 0.1 were considered as significant. Differentially activated ligand-receptor pairs between groups were visualized by dotplot in ggplot2.

RESULTS

Clinical benefit characteristics

Follow-up of the patient after treatment to six months, each four weeks the patient was asked to physical examination and CT showed the major tumor was significantly smaller than before treatment, major mass is smaller from 56mm x 38mm to 14 mm x 26mm, the size of the tumor is shrinking from many angles (Figure 2A to 2I).

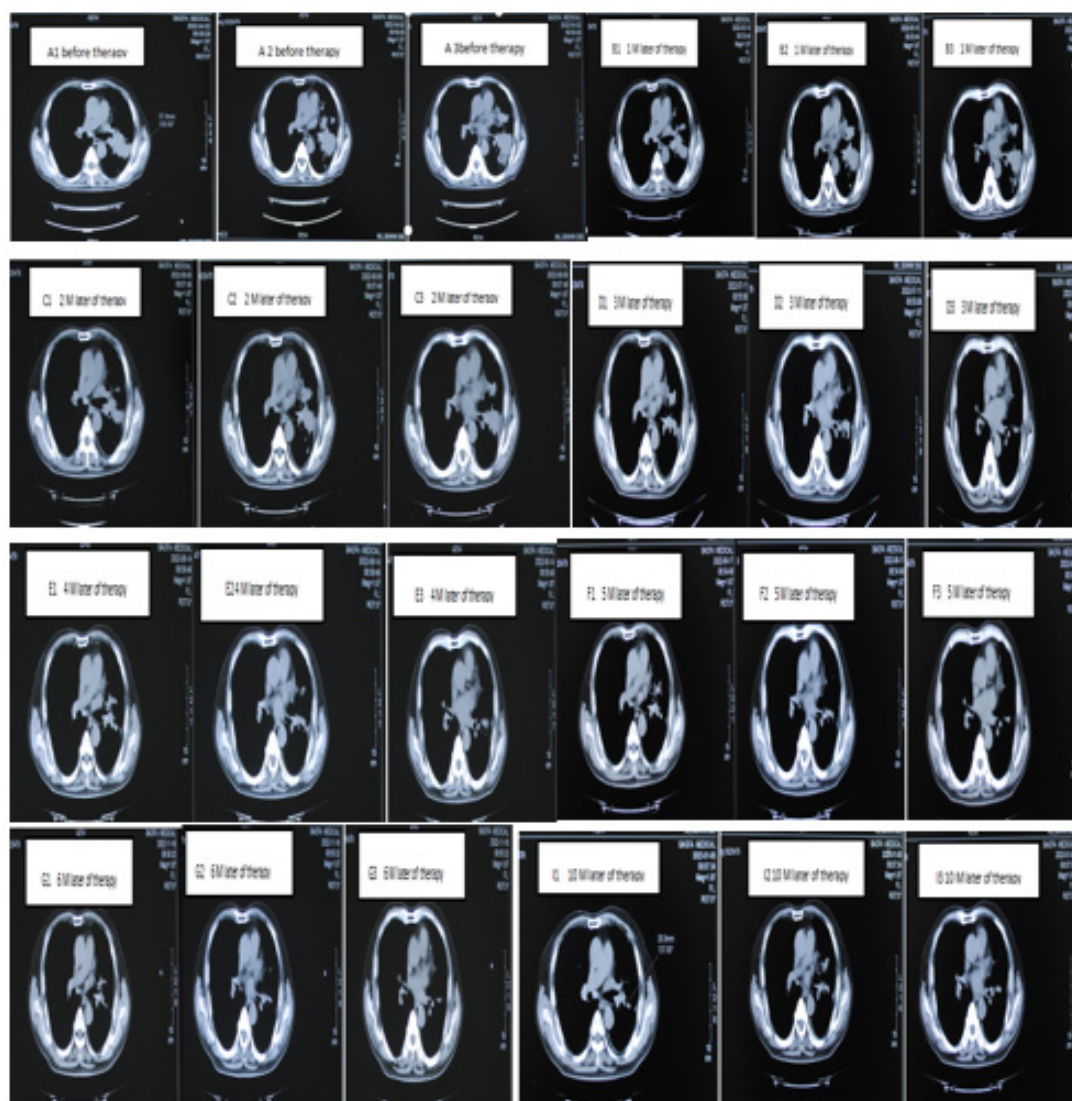


Figure 2: Lung cancer patient's CT showed tumor size before and after treatment of HELC and PD-1 treatment, it showed tumor significantly shrinkage, the size of the tumors including untreated tumors is shrinking at multiple slides of CTs (A) 1,2,3 were the patient's CT before treatment; (B) 1,2,3 were the 1 months after treatment; (C) 1,2,3 were the 2 months after treatment; (D) 1,2,3 were the 3 months after treatment; (E) 1,2,3 were the 4 months after treatment; (F) 1,2,3 were the 5 months after treatment; (G) 1,2,3 were the 6 months after treatment; (I) 1,2,3 were the 10 months after treatment.

Landscape of single cell transcriptome sequencing before and after lung cancer treatment

The cluster analysis of this test obtained 7 subsets from lung tumor sample in a total of 20925 cells, these include B cells, Epithelial cells, Fibroblasts, Mononuclear Phagocytes (MPs), Mast cells, Neutrophils, T and NK cells, at the same time, the proportion of Epithelial cells, MPs and Fibroblasts decreased in LC_A sample compared with LC_B sample, while the proportion of Neutrophils, T and NK cells and B cells was higher. It was found that two subtypes with expression of heat map of top 10 differential genes, including Alveolar Type II (AT2), cancer

cells were obtained with a total of 6929 cells, the proportion of cancer cells in LC_A sample decreased while the proportion of AT2 cells increased. Also analysis of cancer cell CNV score: LC_A sample has a lower CNV score, which indicates that compared with LC_B sample, the malignant degree of LC_A samples is low, while analysis of tumor heterogeneity in cancer cell compared with LC_B, the score of LC_A sample is lower, and the data show that the malignant degree of LC_A samples was low compared with LC_B sample the gene difference analysis of cancer cell showed that LC_B sample was higher than LC_A sample S100A11, S100A8 and S100A9 are highly express (Figure 3A to 3C).

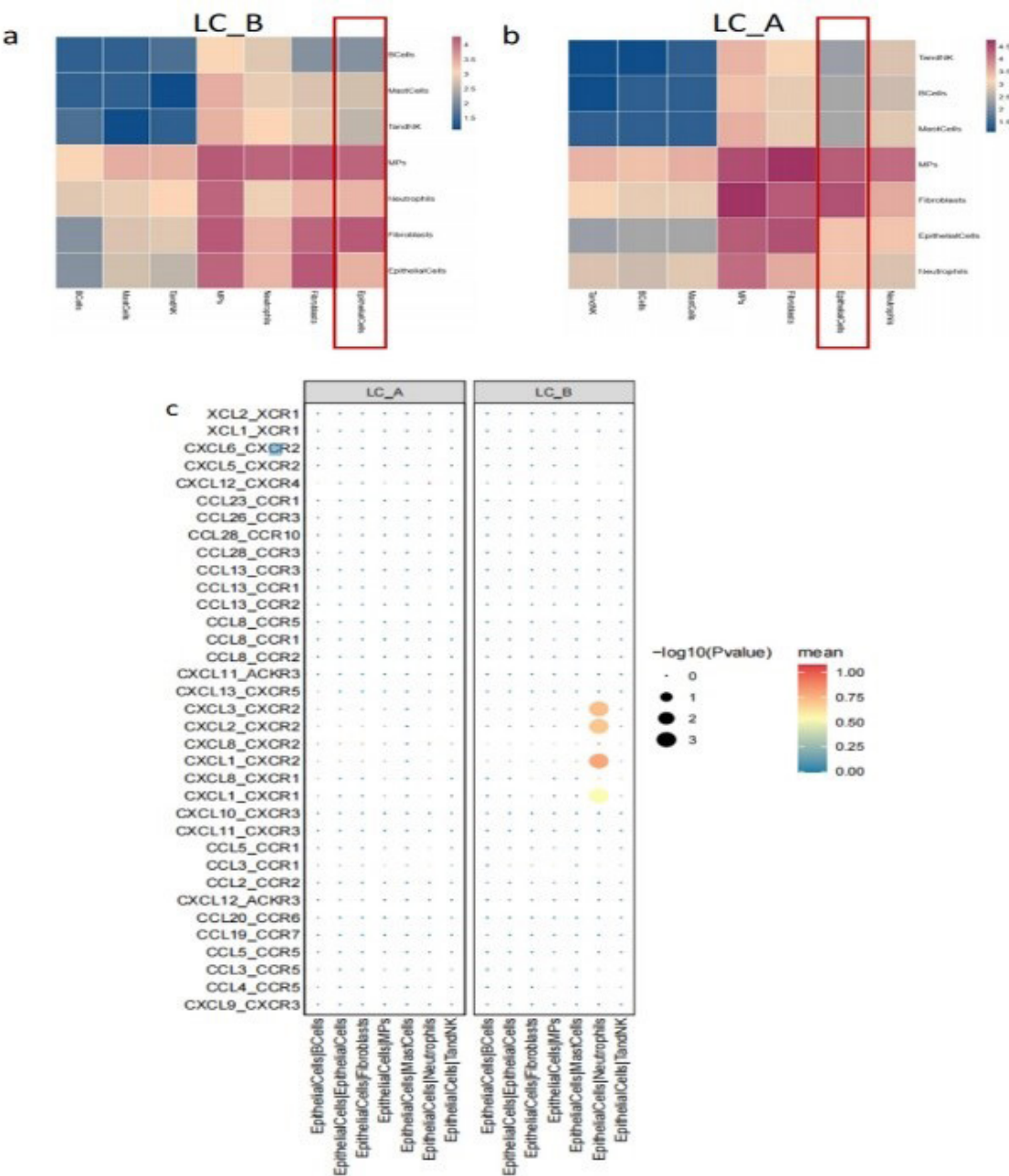


Figure 3: There is a strong link between cells in lung cancer patients before and after treatment Inflammation and fibrosis (A,B) Compared with LC_A sample, in LC_B sample, Epithelial cells and Fibroblasts interact less logarithmically, Epithelial cells and MPs interact logarithmically, but Epithelial cells and Neutrophils interact logarithmically; (C) Bubble map of chemokine ligand pairs: Compared with LC_A samples, LC_B samples, Epithelial cells and Neutrophils were investigated with CXCL3_CXCR2, CXCL2_CXCR2 and CXCL1_CXCR2 received strong ligand pairs.

Single-cell transcriptome profile of lung sample after lung cancer treatment

We performed scRNA-seq for samples of lung cancer before and after lung tumor treated of HELC. According to the scRNA-seq experimental design, the viable single cells was gotten from fresh tissue samples.

Landscape of global transcriptome characteristics of lung tumor samples before and after lung major cancer treated with cytotoxic drug plus hapten

After standard data preprocessing and quality control, we obtained 20925 cells' RNA transcription profiles. By normalizing gene expression profiles, principal component analysis, and graph-based clustering methods, 7 cell populations was identified. Using canonical cell-type markers, we annotated the obtained cell populations into three major

categories: B cells, Epithelial cells, Fibroblasts, Mononuclear Phagocytes, Mast cells, Neutrophils, T and NK cells. Single cell scRNA-sq was performed on two samples of lung cancer before and after lung tumor treatment of HELC, and a total of 7 cells populations were obtained by dimensionality reduction clustering. The cell types were annotated according to the top 10 marker gene of each cell. Tumor copy number variation analysis (CNV) showed obvious copy number variation in epithelial cells with Conducted CNV analysis with reference to T and NK cell, such as increased number of insertions on chromosome, and large number of fragment deletions on chromosome. Therefore, epithelial cells were identified as malignant cells in sample of LC_B, and AT2 cells appears excepted epithelial cells in sample of LC_A. The score of lung cancer cell malignancy showed that the cell malignancy was relatively low after treatment (Figure 4A to 4D and 5A to 5F).

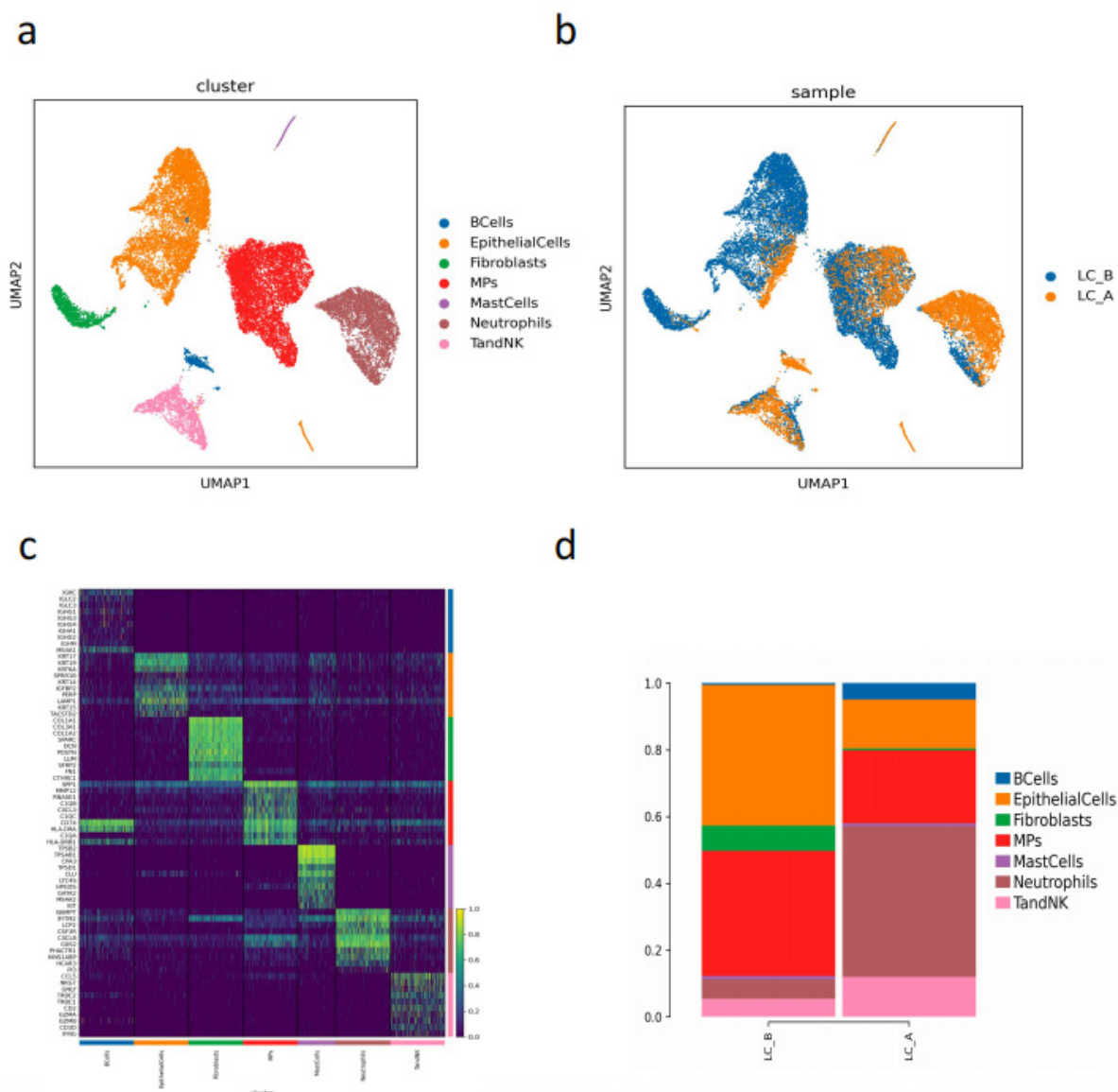


Figure 4: Global transcriptome landscape of lung cancer before and after lung cancer treated with hapten hanced intratumoral injection with cyctooxic drug plus hapten with total cell in 20925. (A) The UMAP cell cluster was formed by dimensional-reduction clustering, and a total of 7 cell types were obtained, including B cells, Epithelial cells, Fibroblasts, Mononuclear phagocytes, Mast cells, Neutrophils, T and NK cells. Different colors represent different cell types; (B) The distribution of various cell types before and after treatment, with blue representing before treatment and yellow representing after treatment; (C) Heat map of marker genes of top 10 genes in each cell type; (D) Histogram of the proportion of various cell types before and after treatment and showed the Neutrophils and B cells dramatic increased. . **Note:** (■) BCells; (■) Epithelial Cells; (■) Fibroblasts; (■) Mast Cells; (■) Neutrophils; (■) T and NK cells

Changes of MPs groups in patients with lung cancer before and after treatment

In the study, there were 6603 MPs cells in total, and two subtypes were obtained, including conventional type 2 dendritic cells, macrophages. Macrophages consist of 6554 cells. In addition, it was observed that GO/KEGG enrichment analysis: Macrophages_NUPR1 finds T cell

activation, Major Histocompatibility Complex (MHC II) signaling pathway down-regulated, and antigen processing and presentation signal down-regulated. T cell activation, MHC II signaling pathway and phagosome signaling are up-regulated in Macrophages_FCN1; Macrophages_HSPA6 involves the up-regulation of ribosome, RNA transcription, antigen processing and presentation signals (Figure 5F to 5K).

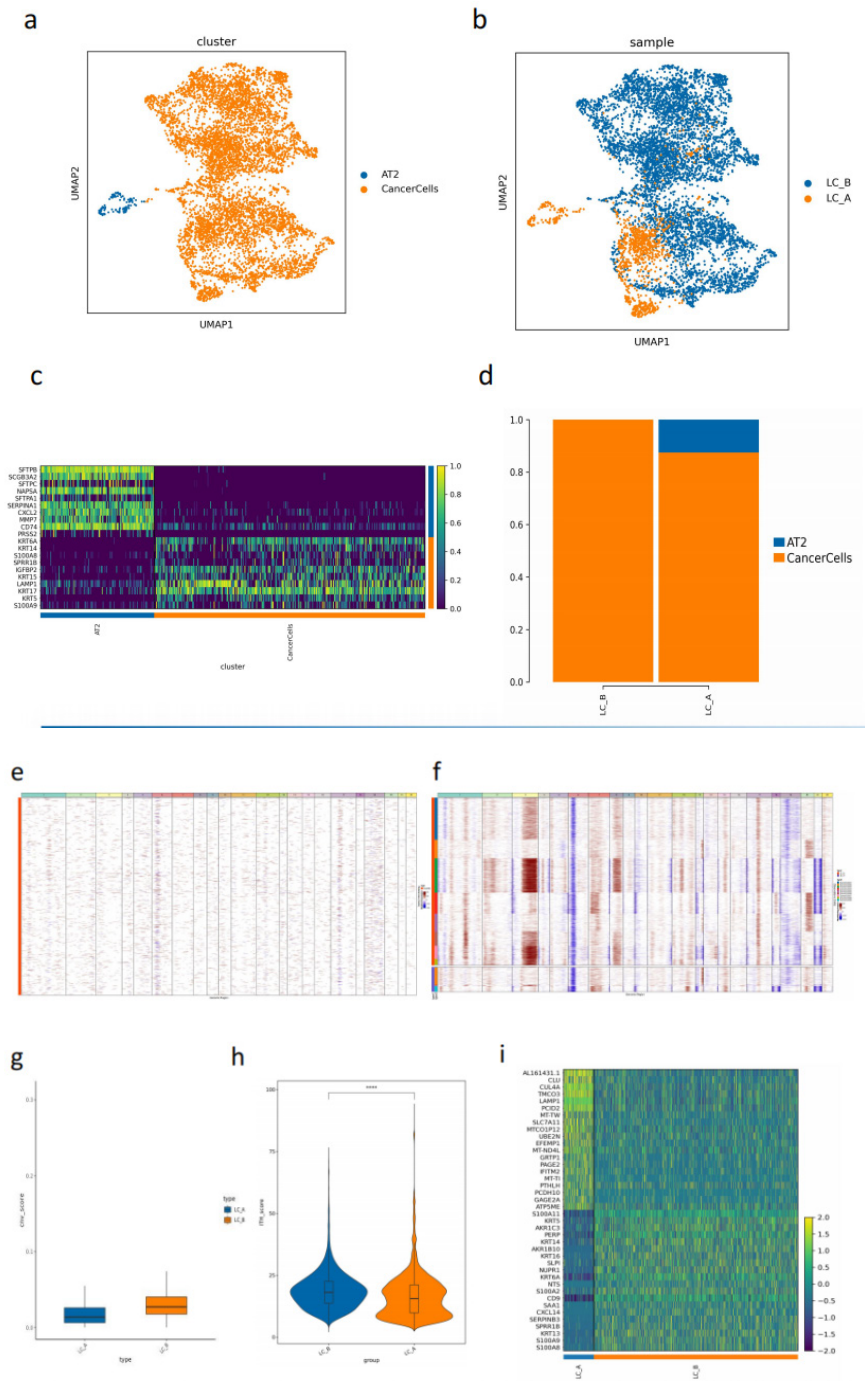


Figure 5: Changes of tumor cell composition in patients with lung cancer before and after treatment (A) Colored UMAP by cell type: Comments on Epithelial cells segmentation Two subtypes, including Alveolar type II (AT2), were obtained with a total of 6929 cells, cancer cells; (B) Colored UMAP according to samples: LC_A samples with AT2 cell sub population are more than LC_B samples; (C) Heat map of top10 differential genes; (D) Histogram of cell proportion: cancer cell in LC_B sample was higher than LC_A sample: the proportion of cancer cells in LC_A sample decreased while the proportion of AT2 cells increased; (E) Conducted CNV analysis with reference to T and NK cell;(F) Heat map for cancer cell inferCNV: LC_B Chromosome increase or deletion is more obvious compared with LC_A sample; (G) analysis of cancer cell CNV score: LC_A sample has a lower CNV score, which indicates that compared with LC_B sample, the malignant degree of LC_A samples is low; (H) Analysis of tumor heterogeneity in cancer cell ITH compared with LC_B, the ITH score of LC_A sample is lower, and the data show that the malignant degree of LC_A samples was low compared with LC_B sample; (I) gene difference analysis of cancer cell showed that LC_B sample was higher than LC_A sample S100A11, S100A8 and S100A9 are highly expressed.

Changes of neutrophil and T & NK in lung tumor before and after lung cancer treatment

While the lung tumor cells were damaged or killed by cytotoxic drug intratumoral, acute inflammation in tumor induced like an immune storm, a massive lymphocyte infiltration into tumor, local edema, became a traditional inflammation. Different neutrophils subtypes were obtained by subdivision annotation in a total of 3315 cells, including Neutrophils1, Neutrophils2, Neutrophils3, Neutrophils4. The proportion of Neutrophils1, Neutrophils3 and Neutrophils4 cells increased and Neutrophils2 cells decreased; comparatively, Neutrophils2 is predifferentiated, the posterior end of Neutrophils1, 3 and 4 was differentiated. The neutrophils2 of LC_A sample decreased compared with that of LC_B sample, and the neutrophilS2 of LC_A sample decreased in LC_B sample, Neutrophils were more at the end of differentiation (Figure 6A to 6I).

It is like acute inflammation as immune storm. Here, hapten interaction with tumor antigens, it was found that T and NK cells from total 1384 cells included, subdivided notes yielded 5 distinct subtypes, including CD8+ effector T cells (CD8TEFF), CD8+ tissue-resident memory T

cells (CD8Trm), Natural Killer cells (NK), naive T cells, regulatory T cells (Tregs), CD8+ effector T cells, CD8Trm and Naive T, increased while Treg decreased. GO enrichment of T and NK cells, compared with LC_B, the NADH-related signals in LC_A samples were down-regulated, and lactic acid was reported to pass The NAD(H) REDOX state limits T cell proliferation; GO enrichment of T and NK cells, compared with LC_B, LC_A sample T cell receptor binding signal is up-regulated [13]. The B cell gene higher expression of CCR7 compared with LC_B samples, and GO/KEGG enrichment analysis between groups: LC_A samples were down-regulated in NADh-related signals, and in chemically-carcinogenic reactive oxygen species (Figure 7A to 7F and Figure 8A to 8E).

Changes of fibroblast composition in patients with lung cancer before and after treatment

LC_A of sample is composed of fibroblasts2, fibroblasts3 and fibroblasts4 in total 1054 cells after lung cancer treatment accounted for the highest proportion compared to LC_B and down-regulation of ECM-receptor interaction signals in fibroblasts2 and fibroblasts3 (Figure 9A to 9E).

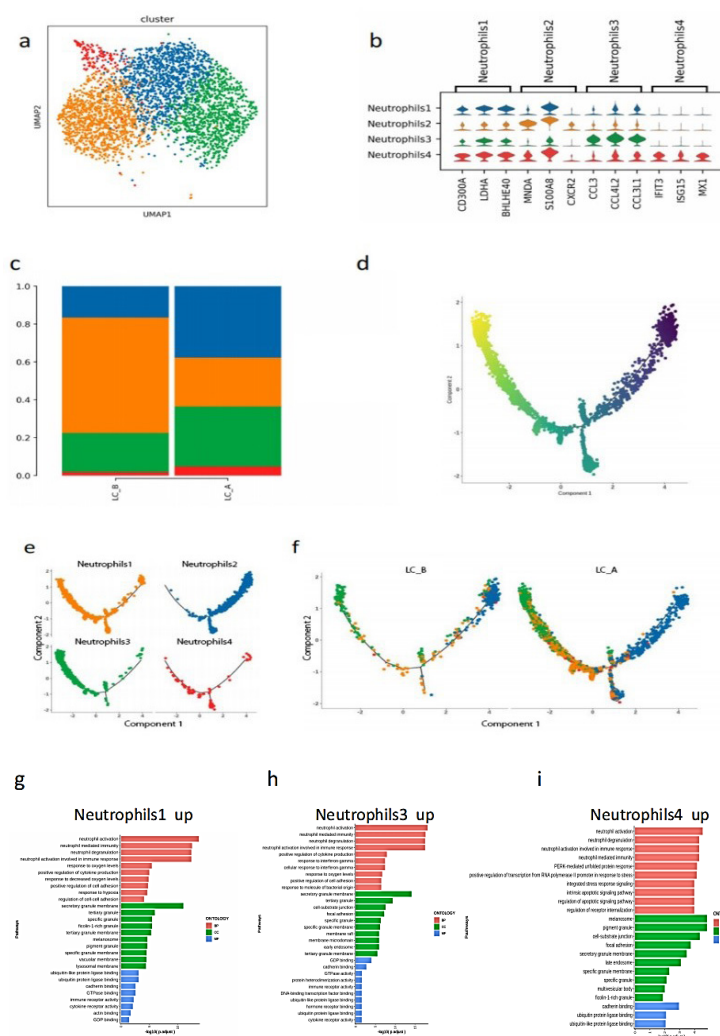


Figure 6: Changes of neutrophil groups in patients with lung cancer before and after treatment. (A) Colored UMAP by cell type: 4 different subtypes were obtained by subdivision annotation. A total of 3315 cells, including Neutrophils1, Neutrophils2, Neutrophils3, Neutrophils4. (B) Violin diagram of top3 differential genes; (C) Cell proportion bar chart: LC_A sample compared with LC_B sample, the proportion of Neutrophils1, Neutrophils3 and Neutrophils4 cells increased. The proportion of Neutrophils2 cells decreased; (D): Pseudo-temporal analysis according to cell type colouring diagram: relative Neutrophils2 is predifferentiated; The posterior end of Neutrophils1, 3 and 4 was differentiated; The Neutrophils2 of LC_A sample decreased compared with that of LC_B sample, and the neutrophilS2 of LC_A sample decreased. In LC_B sample, Neutrophils were more at the end of differentiation. **Note:** (E) Neutrophils1; (F) Neutrophils2; (G) Neutrophils3; (H) Neutrophils4

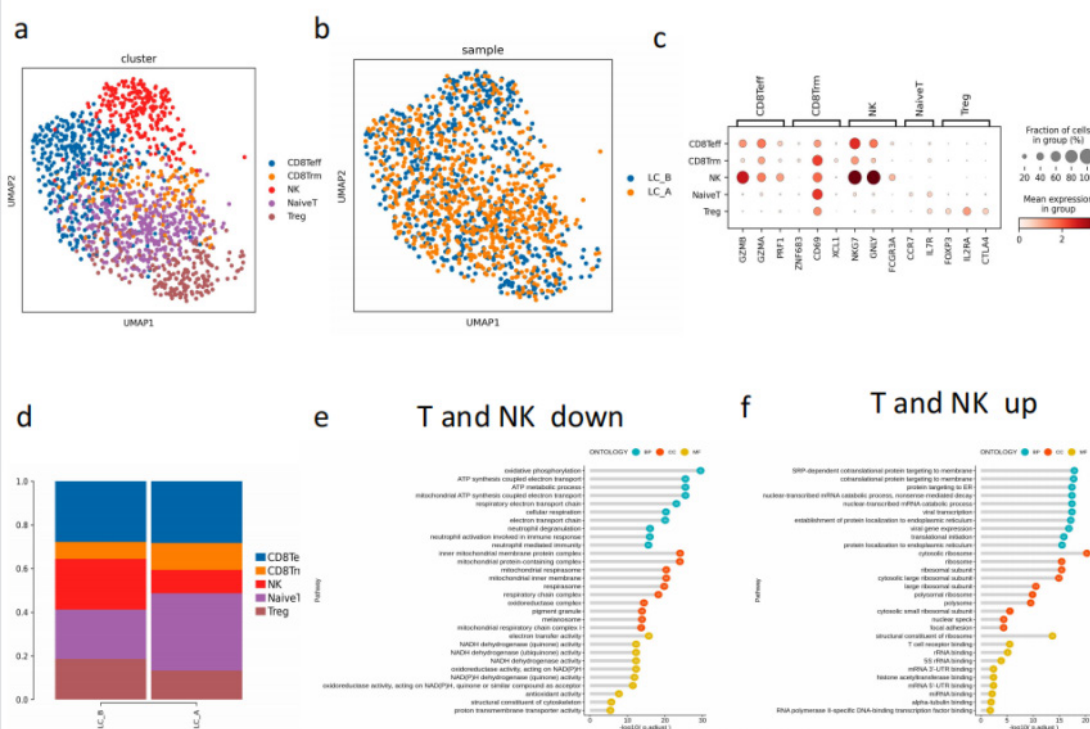


Figure 7: Changes of T and NK cell of composition in patients with lung cancer before and after treatment. (A) Colored UMAP by cell type: T and NK cells total 1384 cells, subdivided notes yielded 5 distinct subtypes, including CD8+ effector T cells, CD8+ tissue-resident memory T cells, Natural killer cells, Naive T cells, Regulatory T cells; (B) Colored UMAP by sample; (C) top3 Marker gene DotPlot; (D) Histogram of cell proportion: LC_A sample was higher than LC_B sample, the proportion of Treg decreased, and the proportion of Naive T and CD8 Trm cells increased; (E) GO enrichment of T and NK cells, compared with LC_B, the NADH-related signals in LC_A samples were down-regulated, and lactic acid was reported to pass The NAD(H) REDOX state limits T cell proliferation; (F) GO enrichment of T and NK cells, compared with LC_B, LC_A sample T cell receptor binding signal is up-regulated. . Note: (●) CD8Teff; (●) CD8Trm; (●) NK; (●) NaiveT; (●) Treg

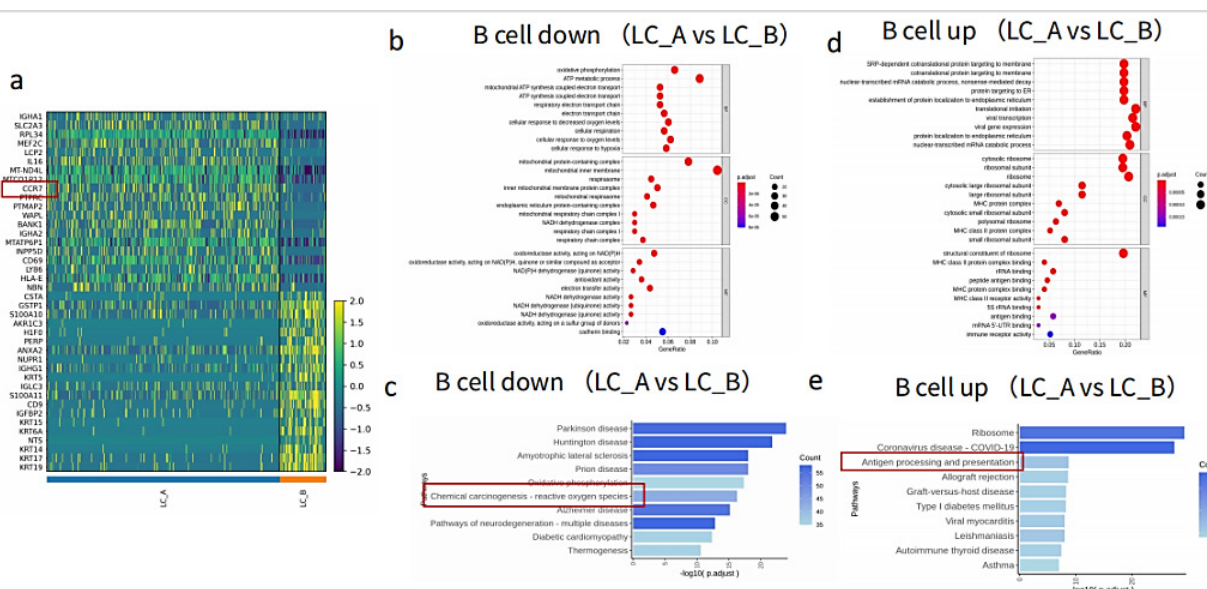


Figure 8: Analysis of B gene Differences between Groups (A) LC_A samples showed higher expression of CCR7 compared with LC_B samples; (B,C) GO/KEGG enrichment analysis between groups: GO analysis results showed that LC_A samples were down-regulated in NADH-related signals, and KEGG enrichment results were down-regulated in chemically-carcinogenic reactive oxygen species; (D) inter-group GO/KEGG enrichment analysis; (E) GO analysis results showed that LC_A samples were up-regulated in MHC-related signals compared with LC_B samples, while KEGG enrichment results showed up-regulated antigen presentation related signals.

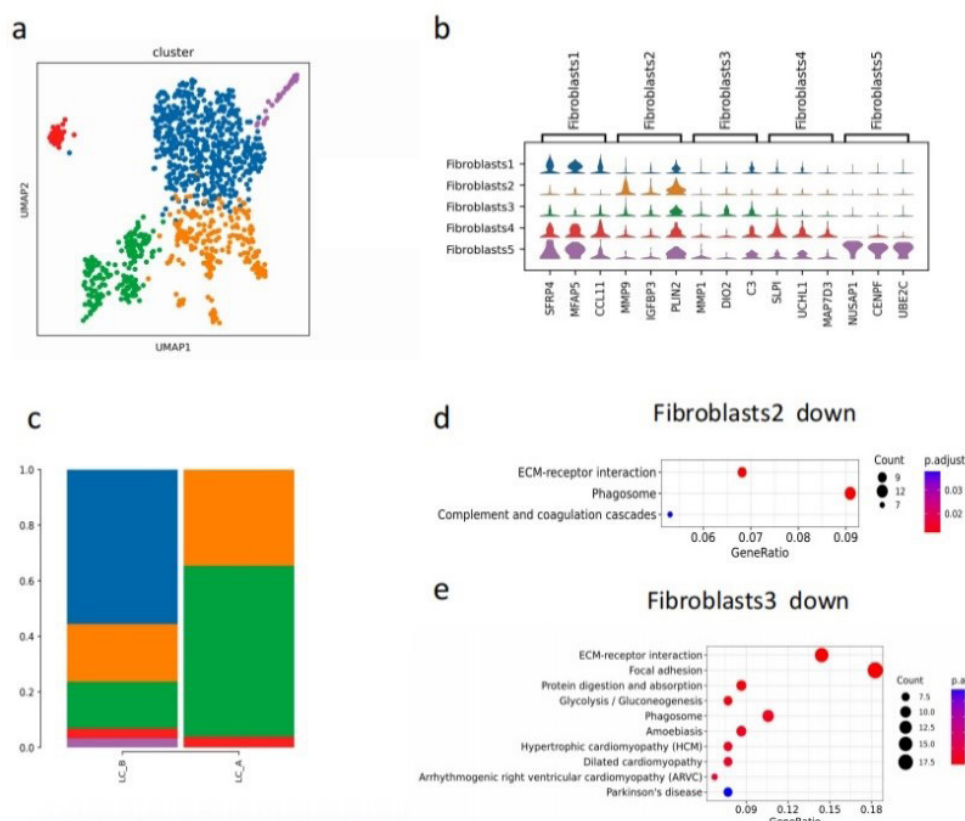


Figure 9: Changes of fibroblast composition in patients with lung cancer before and after treatment. (A) Colored UMAP by cell type: a total of 1054 cells were clustered unsupervised, Fibroblasts1, Fibroblasts2, Fibroblasts3, Fibroblasts4, Fibroblasts5; (B) Violin diagram of top3 Differential Genes; (C) cell proportion bar chart: LC_A sample compared with LC_B sample's Fibroblasts2, Fibroblasts3 cells occupy more; LC_B sample consists of Fibroblasts1, Fibroblasts2, Fibroblasts3, Fibroblasts4, Fibroblasts5, LC_A sample is composed of Fibroblasts2, Fibroblasts3 and Fibroblasts4; (D,E) KEGG enrichment analysis: down-regulation of ECM-receptor interaction signals in Fibroblasts2 and Fibroblasts3. **Note:** (Blue) Fibroblasts1; (Orange) Fibroblasts2; (Green) Fibroblast3; (Red) Fibroblasts4; (Purple) Fibroblasts5

DISCUSSION

Lung cancer is the leading cause of cancer death in the United States. The scientific treatment of non-small cell lung cancer (NSCLC) has made significant progress over the past decade. More are detected early because of screening. The National Lung Screening Trial found that screening high-risk groups using low-dose chest computed tomography reduced lung cancer mortality by 20 percent and all-cause mortality by 6.7 percent. Treatment options for lung cancer have also been developed with the introduction of several tyrosine kinase inhibitors in patients with EGFR, ALK, ROS1, and NTRK mutations. Similarly, more interestingly, Immune Checkpoint Inhibitors (ICIs) have dramatically changed the treatment landscape for NSCLC [14]. However, despite the success of ICIs, resistance to these agents restricts the number of patients able to achieve durable responses, and immune-related adverse events complicate treatment. Thus, a better understanding of the requirements for an effective and safe antitumor immune response following ICIs therapy is needed [15].

ICIs with chemotherapy drug and other agents like anti-angiogenic agents, or design new immunotherapies as a options for the treatment of late stages of lung cancer showing interesting benefit of patient [15,16]. Local treatment with hapten like HELC, awaking the immune system of the host into the recognition and sensitization in advance and fighting posture to tumor cells, it could be improve the ICIs more efficacy as an new option, there is few report using local therapy combination with ICIs. Local tumor treatment of HELC has advantages

of killing tumor and haptenation with tumor associate antigens to a neu tumor associate antigen and induced immune strong reaction, being adjuvant therapy has achieved some success for most of late stages of lung cancer patients [4-6]. Hapten is an immune modulator to modified tumor epitope of tumor antigens from death tumor cells killed by cytotoxic drug and became to a neu tumor associate antigen [5,6]. All immunity reaction is related the abscopal effect. Over the past century, many scientists have dreamed of using the lock-in of abscopal effect, an immunity reaction, to control tumors distal to the primary tumor, but failed due to unknown mechanisms and limited methods, now ICIs is a great option to improve the abscopal effect or abscopal may improve the ICIs efficacy. In order to get an understanding of this study, awaken the immune cell for ready cancer immunotherapy, we investigated the molecular changes of untreated tumor reflection from the lung cancer before and after intra-tumoral injection with cytotoxic drugs plus hapten. Token of both samples of sentinel lymph nodes were further analyzed by scRNA-seq while gave the patient normal dose of PD1 therapy only twice treatment HELC with successful response.

After the treatment, immunity reaction starts in the body, MPs, mature DC cells present a higher capacity of antigen presentation by MHC II signaling pathway, while macrophage and monocyte did so by MHC I. The cluster analysis of this test was obtained 7 subsets from lung tumor sample, a total of 20925 cells, these include B cells, Epithelial cells, Fibroblasts, Mononuclear Phagocytes (MPs), Mast cells, Neutrophils, T and NK cells. The tumor cells have decreased while immune cells of Mast cell, Mononuclear Phagocytes, Neutrophils, T and NK cells

significantly increased and occupied the distribution of total cells as majority, also top of 10 genes with higher expression. Then immune cells may be activated and start to proliferate and differentiate into effector T or B cells or NK cells that secrete cytokines and play a role in anti-tumor immunity. After one week of first treatment, biopsies were taken again from lung tumor, the cancer cell with low activity less than 12.55% while the epithelium of lung was significantly reduced. It showed that lung cancer cell dies mostly, left over small part of lung cancer cells. The cell types were annotated according to the top 10 marker gene of each cell (Figure 4 and Figure 8).

Our study is a cytotoxic drug injected into tumor with hapten to modifying released tumor antigens is presented to T cells by antigen presenting cells, here Tumor Associate Antigen (TAA) modified by hapten as neu antigens, when MPs meet the neu antigens, MPs could change to be DC for playing the function of antigen presenting, further

produce new T cells to fight the distal tumor cells. Tumor copy number variation analysis (CNV) showed obvious copy number variation in epithelial cells with conducted CNV analysis with reference to T and NK cell, such as increased number of insertions on chromosome, and large number of fragment deletions on chromosome (Figure 5E and 5F). In the study, MPS subtype was divided into two conventional type 2 dendritic cells and macrophages; Macrophages is summarized as an unsupervised cluster. It is divided into 7 heterogeneous subgroups. They are Macrophages_NUPR1, Macrophages_IL1B and Macrophages_C1QB, Macrophages_HSPA6, Macrophages_MKI67, Macrophages_FCN1, and Macrophages_MMP7. In addition, it was observed that GO/KEGG enrichment analysis: Macrophages_NUPR1 finds T cell activation, MHC signaling pathway down-regulated, and antigen processing and presentation signal down-regulated (Figure 10A to 10E).

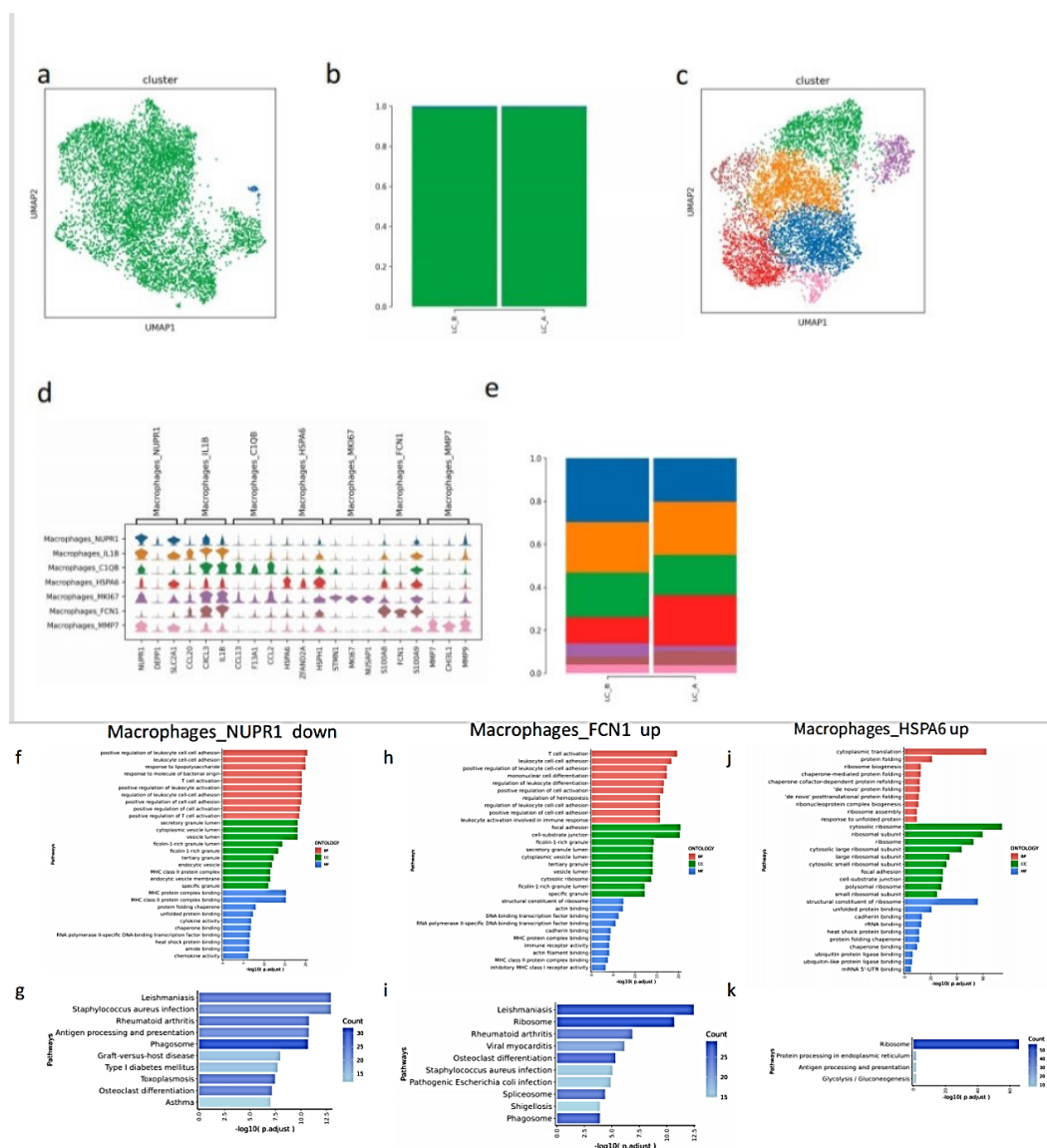


Figure 10: Changes of MPs groups in patients with lung cancer before and after treatment. (A) UMAP colored by cell type: MPs totaled 6603 cells, subdivision notes obtained two different subtypes, including conventional type 2 dendritic cells, macrophages; (B) Bar chart of cell proportion: LC_A and LC_B samples were all Macrophages dominate; (C) map: Macrophages a total of 6554 cells, the unsupervised cluster was divided into 7 heterogeneous subgroups. Macrophages_NUPR1, Macrophages_IL1B, Macrophages_C1QB, Macrophages_HSPA6, Macrophages_MKI67, Macrophages_FCN1, Macrophages_MMP7; (D): Violin diagram of top 3 differential genes; (E) Histogram of cell proportion: compared with LC_B sample, LC_A sample with the cells of Macrophages_HSPA6 and Macrophages_FCN1 were obvious high, The proportion of Macrophages_NUPR1 is obviously increased in LC_B sample, while macrophages_nupr1 showed a downward trend in LC_A sample. **Note:** (●) Macrophages_NUPR1; (■) Macrophages_IL1B; (■) Macrophages_HSPA6; (■) Macrophages_C1QB; (■) Macrophages_MKI67; (■) Macrophages_FCN1; (■) Macrophages_MMP7

It was found that T and NK cells from total 1384 cells included, subdivided notes yielded 5 distinct subtypes, including CD8⁺ effector T cells, CD8⁺ T_{RM}, NK cells, naive T cells, regulatory T cells; memory T cells, CD8⁺ effector T cells, CD8⁺ T_{RM} and Naive T increased in LC_A sample while Treg decreased in LC_B sample (Figure 7A to 7D). Above characteristic of inflammation showed this inflammation is a special inflammation, like vaccine manufacturer to produce the D8⁺ effector T cells, CD8⁺ T_{RM}, natural killer cells, naive T cells.

CONCLUSION

Patient with metastasis lung cancer had a quickly response for PD1, tumor shrink from 56mm x 38mm to 14 mm x 26mm, the size of the tumors including untreated tumors is shrinking at multiple levels, the quality of life has improved significantly and KPS score from 56 to 87. In this study, the increases of CD8⁺ T cells and CD8⁺ T_{RM} are playing an important role in patient self-immunotherapy and it improved the basic intracellular milieu for PD1 therapy. Awakening immune cell by HELC can induce an abscopal effect due to the CD8⁺ effector T cells endowed with certain functions of targeting recognition to tumor cells, out of WtO condition, and make immune cells ready for ICIs to activate the CD8⁺ effector T cells in sensitized state, so that abscopal effect and ICIs can mutual support to produce more efficacy in cancer immunotherapy, it may provide a new option in treating all of late stages cancers.

DECLARATION

Conflict of interest statement

All of the authors do not have any conflict interest concerning this research.

Translational relevance to the manuscript

This research is highly practice valuable for medical translational relevance to the manuscript and it may be a precision immuno-therapy for all of solid tumors.

Highlights

Significance of immunity reaction observed at molecular level in untreated tumors from major tumor hapten enhanced local chemotherapy which is rarely studied by single-cell scRNA-seq and comparison with the molecular changes of untreated tumor before and after the major tumor treated with cytotoxic drug plus hapten, it may wake up the immune cells to ready of cancer immunotherapy

REFERENCES

1. Oliver AL. Lung cancer: Epidemiology and screening. *Surg Clin North Am.* 2022;102:335-44.
2. Patel SA and Weiss J. Advances in the treatment of non-small cell lung cancer: immunotherapy. *Clin Chest Med.* 2020;41:237-47.
3. Cortiula F, Reymen B, Peters S, et al. Immunotherapy in unresectable stage III non-small-cell lung cancer: state of the art and novel therapeutic approaches. *Ann Oncol.* 2022;33:893-908.
4. Yu B, Lu Y, Gao F, et al. Hapten-enhanced therapeutic effect in advanced stages of lung cancer by ultra-minimum incision personalized intratumoral chemoimmunotherapy therapy. *Lung Cancer (Auckl).* 2015;6: 1-11.
5. Jing P, Liu J, Li J, et al. Hapten improved overall survival benefit in late stages of non-small cell lung cancer (NSCLC) by ultra-minimum incision personalized intratumoral chemo immunotherapy (UMIPIC) therapy with and without radiation therapy. *J Cancer Prev Curr Res.* 2016;4: 119-22.
6. Yu B, Fu Q, Han Y, et al. An acute inflammation with special expression of CD11 & CD4 produces abscopal effect by intramoral injection chemotherapy drug with hapten in animal model. *J Immunological Sci.* 2022;6: 1-9.
7. Abuodeh Y, Venkat P and Kim S. Systematic review of case reports on the abscopal effect. *Curr Probl Cancer* 2016;40: 25-37.
8. Kechin A, Boyarskikh U, Kel A, et al. cutPrimers: A new tool for accurate cutting of primers from reads of targeted next generation sequencing. *J Comput Biol.* 2017;24: 1138-43.
9. Dobin A, Davis CA, Schlesinger F, et al. STAR: ultrafast universal RNA-seq aligner. *Bioinformatics.* 2013;29: 15-21.
10. Yu G, Wang L, Han Y, et al. cluster Profiler: An R package for comparing biological themes among gene clusters. *OMICS: A J Integr Bio.* 2012;16: 284-87.
11. Qiu X, Hill A, Packer J, et al. Single-cell mRNA quantification and differential analysis with Census. *Nat Method.* 2017;14:309-15.
12. Efremova M, Tormo MV, Teichmann SA, et al. CellPhoneDB: inferring cell-cell communication from combined expression of multi-subunit ligand-receptor complexes. *Nat Protoc.* 2020;15: 1484-506.
13. Quinn WJ, Jing J, TeSlaa T, et al. Lactate limits T cell proliferation via the NAD(H) redox state. *Cell Rep.* 2015;33: 108500.
14. Duma N, Davila RS and Molina JR. Non-small cell lung cancer: Epidemiology, screening, diagnosis, and treatment. *Mayo Clin Proc.* 2019;94:1623-40.
15. Bagchi S, Yuan R and Engleman EG. Immune checkpoint inhibitors for the treatment of cancer: clinical impact and mechanisms of response and resistance. *Annu Rev Pathol.* 2021;16: 223-49.
16. Song Y, Fu Y, Xie Q, et al. Anti-angiogenic agents in combination with immune checkpoint inhibitors: A promising strategy for cancer treatment. *Front Immunol* 2020;11: 1956.